Critical flux pinning and enhanced upper critical field in magnesium diboride films

Milind N. Kunchur,* Cheng Wu, Daniel H. Arcos, and Boris I. Ivlev[†]

Department of Physics and Astronomy, University of South Carolina, Columbia, South Carolina 29208, USA

Eun-Mi Choi, Kijoon H. P. Kim, W. N. Kang, and Sung-Ik Lee

National Creative Research Initiative, Center for Superconductivity and Department of Physics, Pohang University of Science and Technology, Pohang 790-784, Republic of Korea

(Received 5 May 2003; published 12 September 2003)

We have conducted pulsed transport measurements on c-axis-oriented magnesium diboride films over the entire relevant ranges of magnetic field $0 \lesssim H \lesssim H_{c2}$ (where H_{c2} is the upper critical field) and current density $0 \lesssim j \lesssim j_d$ (where $j_d \sim 10^7$ A/cm^2 is the depairing current density). The intrinsic disorder of the films combined with the large coherence length and three dimensionality, compared to cuprate superconductors, results in a sixfold enhancement of H_{c2} (to 17 ± 3 T) and raises the depinning current density j_c to within an order of magnitude of j_d. The current-voltage response has an unusually steep nonlinear shape at all fields, resulting from a combination of depinning and pair breaking, and has no trace of an Ohmic free-flux-flow regime.

I. INTRODUCTION

Magnesium diboride (MgB$_2$) recently made an impact as a promising new superconductor with a surprisingly high critical temperature T_c for a simple binary compound. Besides the temperature T, the other principal parameters that define the operational space of a superconductor are magnetic field H and current density j. Superconductivity perishes above $H_{c2}(T,j)$ and $j_d(T,H)$. For most practical applications it is not sufficient for the system to be merely in a superconducting state (presence of a finite order-parameter amplitude) but the system also needs to be in a dissipationless state (constancy of order-parameter phase difference across sample length). Thus from a practical standpoint, the conventional critical current density j_c is limited by the depinning of vortices and their consequent motion. In the high-T_c cuprates, the large T_c is accompanied by high values[1] of $j_d (>10^8$ A/cm^2). However the layered structure and small coherence length ξ lead to very weak vortex pinning. Thus between j_c and j_d, there can be a broad dissipative regime.[2]

MgB$_2$ has an intermediate T_c and low values of j_d and H_{c2}. $j_d \sim 10^7$ A/cm^2 at low temperatures and, in single crystals, $H_{c2} \sim 3$ T parallel to the c axis.[3] In the films studied here, the intrinsic disorder makes two striking improvements. First of all H_{c2} is enhanced six-fold. Second, pinning is enhanced to the point of raising j_c to the same order of magnitude as j_d. These observations are consistent with the reduction of ξ with disorder. Finally MgB$_2$'s normal-state resistivity ρ_n is lower than that of a typical cuprate superconductor (e.g., Y$_1$Ba$_2$Cu$_3$O$_7$) by two orders of magnitude. This increases the vortex viscosity by the same factor, so that even when the vortices are depinned, they flow at very low velocities causing insignificant dissipation until j_c becomes comparable to j_d. All these factors lead to an extremely steep nonlinear current-voltage (IV) curve with a complete absence of an Ohmic regime characteristic of free flux flow.[4]

II. EXPERIMENTAL DETAILS

The samples are 400-nm-thick films of MgB$_2$ fabricated using a two-step method whose details are described elsewhere.[5,6] An amorphous boron film was deposited on a $(1\bar{1}02)$Al$_2$O$_3$ substrate at room temperature by pulsed-laser ablation. The boron film was put into a Nb tube with high-purity Mg metal (99.9%) and the Nb tube was then sealed using an arc furnace in an argon atmosphere. Finally, the tube was heated to 900 ° C for 30 min in an evacuated quartz ampoule sealed under high vacuum. X-ray diffraction indicates a highly c-axis-oriented crystal structure normal to the substrate surface with no impurity phases. The films were photolithographically patterned down to narrow bridges. In this paper we show data on three bridges, labeled S, M, and L (for small, medium, and large) with lateral dimensions 2.8×33, 3.0×61, and 9.7×172 μm^2, respectively. The lateral dimensions are uncertain by ± 0.7 μm and the thickness by ± 50 nm. Figure 1(a) shows the sample geometry. The horizontal sections of the current leads add a $\sim 15\%$ series resistance to the resistance of the actual bridge, which enters in measurements made at very small j. At high j in the mixed state, the extra contribution is frozen out because the current is spread out in these wider areas, diluting its density, so that one observes mainly the resistance of the bridge (A more intricate contact geometry was prohibited because of the extreme difficulty we faced in etching MgB$_2$).
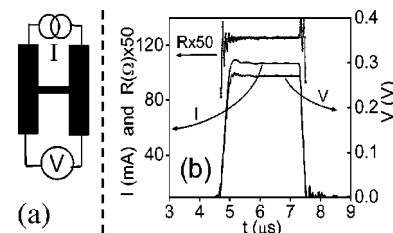

FIG. 1. (a) Sample geometry used for resistance measurement. At low values of j the wide lead areas add a constant resistance of about 15% of the total value. At high j this contribution is frozen out. (b) Pulse waveforms under worst-case conditions ($j = 9.7$ MA/cm^2, $E = 83$ V/cm, and $p = jE = 803$ MW/cm^3 on the plateaus). The resistance rises to (90% of) its final value in about 50 ns from the (10%) onset of I.
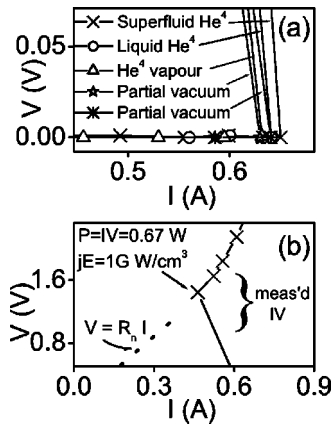
FIG. 2. Zero-field *IV* curves for sample *L* show an abrupt switch to a state of full normal-state resistance R_n by currents of pair-breaking magnitudes. (a) The switch to a dissipative state is not significantly influenced by the thermal environment. (b) Top portion of the curve in superfluid He^4. The resistive portion of the measured curve extrapolates to the $V = R_n I$ dashed line.

FIG. 3. Resistive transitions of two MgB$_2$ bridges at indicated flux densities. $I = 1.4$ μA. (a) Sample *M*; midpoint T_c's lie on the dashed line through $R = R_n/2 = 1.95$ Ω. (b) Similar set for sample S. Dashed lines run through $R = R_n/2 = 1.22$ Ω, and also through the lower and higher resistive criteria $R = 0.84$ Ω and $R = 1.76$ Ω.

The nonlinear electrical transport measurements were made using a pulsed signal source with pulse durations ranging from 0.1 to 4 μs and a duty cycle of about 1 ppm. At the other extreme, a conventional continuous dc method at a very low current ($I = 1.4$ μA) was employed for the resistive traces used to determine H_{c2}. Figure 1(b) shows pulse wave forms under the especially severe conditions of $j = 9.7$ MA/cm^2, $E = 83$ V/cm, and $p = jE = 803$ MW/cm^3. The resistance rises to 90% of its final value in about 50 ns from the 10% onset of *I*. From a knowledge of the thermal conductivities and specific-heat capacities of the film and substrate materials, and their mutual thermal boundary resistance, one can calculate the total thermal resistance R_{th} for any pulse duration.[2,7] Also if $R(T)$ has enough variation, the film's own resistance can be used as a thermometer to measure R_{th}. For films of Y$_1$Ba$_2$Cu$_3$O$_7$ (YBCO) on LaAlO$_3$, which were used for most of our previous work, we found $R_{th} \sim 1$–10 nK cm^3/W at microsecond time scales.[2,8,9] In the case of our MgB$_2$ films, we expect R_{th} to be smaller because of sapphire's very high conductivity. However the five parameters required to calculate R_{th} from first principles are not all known for this film-substrate combination and MgB$_2$ has a very flat $R(T)$ below 50 K, so one cannot measure R_{th} as was done for YBCO. We can, however, obtain an upper bound on R_{th} in the following way: Figure 2(a) shows *IV* curves for sample *L* in zero field (This is the largest sample with the lowest surface-to-volume ratio, so that it represents the worst-case thermal scenario). The curves were measured with the sample in different thermal environments. Above some threshold current $I_d \sim 650$ mA, the system abruptly switches into the normal state. The value of I_d is not sensitive to the thermal environment contacting the exposed surface of the film, confirming that the highly conductive sapphire, together with the greatly reduced heat input during the short pulse, prevents the film's temperature from rising significantly (It has been shown by Stoll *et al.*[10] that if there is sample heating, the thermal environment makes a significant difference because it will provide an additional path for the
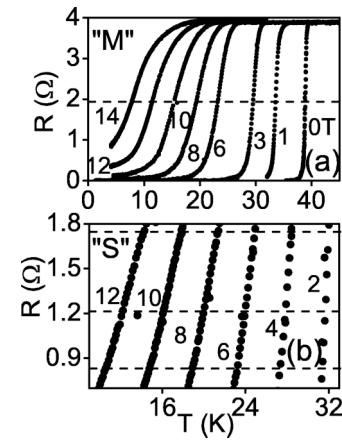
heat to flow through). Figure 2(b) shows the top portion of one of the *IV* curves. The resistance jumps directly to the full normal-state value (The arrow indicates the first data point with nonzero resistance; the dashed line corresponds to $V = R_n I$). It is argued elsewhere[11] that this jump to the normal state occurs due to pair breaking by the current.[12] At the point the system is just driven normal, the power density reaches $p = jE = 1.01$ GW/cm^3 [arrow in Fig. 2(b)]. This sets a gross upperbound of $R_{th} \sim 7$ nK cm^3/W. Note that the main bottleneck of heat conduction is the film-substrate boundary resistance which is not strongly temperature dependent.[7] In the present work, typical p values are two orders of magnitude lower than the critical 1 GW/cm^3 and so we expect the temperature rise to be a small fraction ($\sim 1\%$) of T_c.

The magnetic field is applied normal to the film (parallel to the c axis), and the self-field of the current (<50 G) is much lower than the applied fields used in this work. Further details of the measurement techniques have been published in a previous review paper[2] and other recent papers.[8,9]

III. RESULTS AND ANALYSIS

Figure 3 shows the resistive transitions at a low continuous current of $I = 1.4$ μA in different fixed magnetic fields. Panel (a) shows the full curves for sample *M*, whereas for sample *S* we show the central region of the transition in panel (b). Both full and central views look very similar for all three samples. In the central region, the shifts are approximately parallel, reducing the ambiguity of $H_{c2}(T)$ defined by the transition-midpoint criterion. Figure 4 shows those $H_{c2}(T)$ values. $H_{c2}(T)$ has an unusual linear dependence that departs noticeably from the dashed line of the WHH (Werthamer-Helfand-Hohenberg) function.[13] This observation is consistent with that of a dirty two-gap superconductor.[14] Panel (b) shows $H_{c2}(T)$ for sample *S* defined by other criteria [see Fig. 3(b) above]. Note that the linear dependence is preserved and the slopes (and hence the
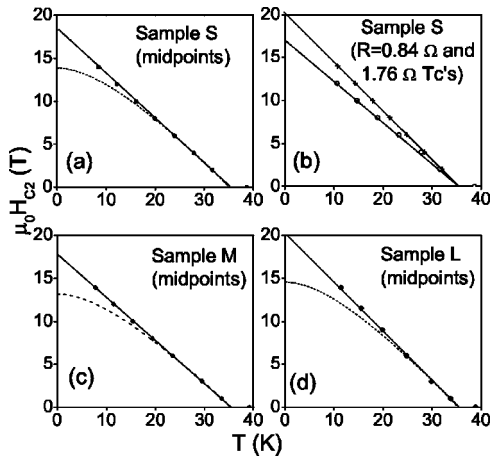
FIG. 4. H_{c2} vs B for three samples. The solid straight lines are linear fits to the data. The dashed lines correspond to the WHH function. Panel (b) shows H_{c2} for sample S defined at two other criteria. The linear behavior of $H_{c2}(T)$ continues to hold for the $R = 0.84 \, \Omega$ and $R = 1.76 \Omega$ criteria.

inferred zero-T values of H_{c2}) do not change significantly with the choice of criteria. We infer a value of 17 ± 3 T for $H_{c2}(0)$, which is six times higher than the value of 3 T found in single crystals.[3] This can be understood in view of the much higher resistivity and hence shorter coherence length ξ: For a dirty superconductor $\xi \approx \sqrt{\xi_0 l}$, where ξ_0 is the clean-limit value of ξ and l is the impurity scattering mean-free-path. Since $\rho \propto l$ and $H_{c2} \propto 1/\xi^2$, we expect $H_{c2} \propto \rho$. The normal resistivity of our film samples (14 $\mu \Omega$ cm) is about seven times higher than the value (2 $\mu \Omega$ cm) of the single crystals of Ref. 3. Note that this H_{c2} enhancement occurs naturally in the as-prepared films without any special effort to introduce pinning sites. The microscopic cause of the enhanced scattering leading to the higher H_{c2} in these samples is presently not clear.

We now turn to the in-field IV curves to investigate the nature of flux motion. In a system with weak flux pinning, the resistance goes through alternate regimes of Ohmic ($V \propto I$) and non-Ohmic behavior. At very low driving forces (low j) there can be observable resistance due to thermally activated flux flow (TAFF) or flux creep. Then one encounters a nonlinear response as current-driven depinning sets in; in effect the number of mobile vortices is rising. This is incipient flux flow. At sufficiently larger j, the vortex motion is effectively free from the influence of pinning and the response becomes Ohmic again. We previously introduced the term *free flux flow* (FFF) for this linear regime.[4] Here the dissipation and resistivity should correspond to the canonical $\rho_f \sim \rho_n B / H_{c2}$ Bardeen-Stephen expression.[15] As one goes beyond FFF, nonlinearity can set in because of heating of the electron gas[8] or changes in the electron distribution function.[16] Finally at yet higher currents, pair breaking destroys superconductivity and drives the system normal. Here the resistance again ceases to change with current, being characteristic of the normal state, and so the response becomes Ohmic one more time. These stages of dissipation have been described in our previous review paper.[2] In $Y_1Ba_2Cu_3O_7$, the depinning critical current is sufficiently
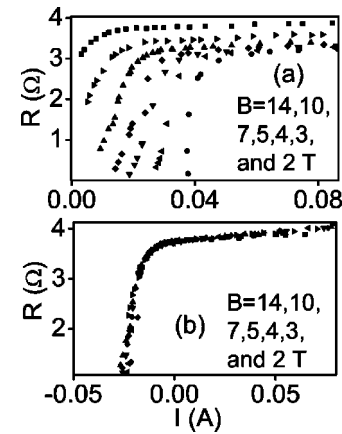

FIG. 5. Resistance vs current curves for sample M. Flux densities are indicated from left to right. The sample was immersed in superfluid helium and $T = 1.5$ K for all data. (a) Raw data. (b) Same data linearly shifted so as to collapse onto a single common curve.

weak compared to the pair-breaking value that all of the regimes can be observed.

In MgB_2 the situation is very different. Figure 5(a) shows the $R(I)$ curves of the present MgB_2 samples. After the onset of dissipation, the resistance quickly rises to the full normal-state value. It should be noted that the plateaus do not correspond to FFF but to the normal state. Accordingly the resistance value changes very little with the applied B, especially for the curves at lower fields.[17] The overall shapes of the curves are almost independent of field. When the
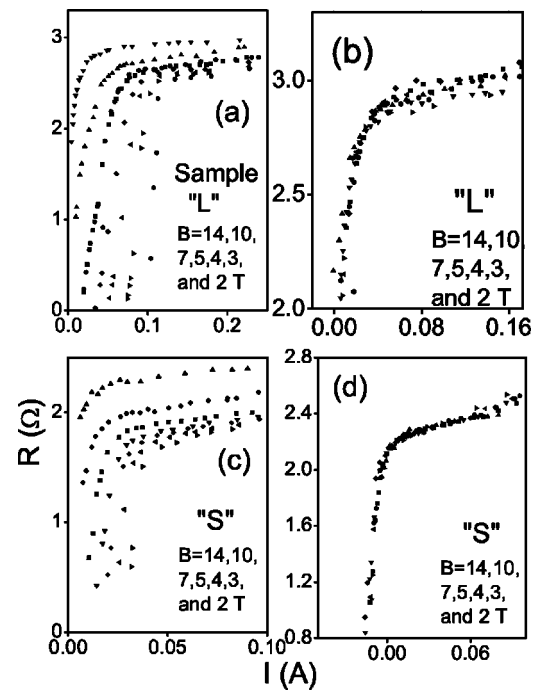

FIG. 6. Resistance vs current curves for samples S and L. Flux densities are indicated from left to right. The sample was immersed in superfluid helium and $T = 1.5$ K for all data. Panels in the left column show raw data and panels in the right column show linearly shifted data.

curves of the previous panels are shifted vertically and horizontally by constant amounts, they can be made to overlap as shown in Fig. 5(b). Figure 6 shows the raw and shifted curves for the other two samples.

These steep *IV* characteristics in MgB_2 are similar to those for niobium alloys, but are markedly different from those in the cuprates. The latter can be understood in terms of MgB_2's lower temperature scale and much greater pinning (due to its higher isotropy and ten times larger vortex cross section). Hence thermal activation and current driven depinning are deferred until j becomes almost comparable to j_d, causing the response to become steeply nonlinear, rising from very little dissipation to the full normal state within a rather narrow range of currents. The collapse in Figs. 6 and 5 seems to suggest that the rise in resistance stems mainly from the intrinsic mechanisms of current- and field-induced pair breaking, rather than from current driven depinning, even when B approaches H_{c2}. This makes MgB_2's mixed-state response unique among studies of type-II superconductors. From the standpoint of applications, this implies that the practically useable current densities are much higher than might be inferred from the j_d of the material, since substantial flux dissipation is deferred until j_c becomes comparable to j_d.

IV. CONCLUSIONS

We have investigated the low-temperature ($T \ll T_c$) in-field transport behavior of MgB_2 and present a measurement of the full dissipation curves (i.e., $0 \leq j \leq j_d$ and $0 \leq R_{T=0} \lesssim R_n$) for this system. MgB_2 films made by the two-step laser-ablation process have an intrinsic pinning of a critical magnitude, such that the principal dissipation and resulting *IV* curves arise mainly from intrinsic mechanisms such as pair breaking. The onset of dissipation is within an order of magnitude of the pair breaking current, even at flux densities of a few teslas—the resistance shows a dramatically steep rise to the full normal-state value as the current is increased beyond j_c. The same disorder that enhances pinning also enhances H_{c2} and qualitatively changes its temperature dependence because of the two-band nature of the superconductivity in this material. As explained by the theory of Gurevich, $H_{c2}(0)$ extrapolates to a higher value than would be expected for WHH behavior, and the slope dH_{c2}/dt is relatively constant. Our measurements of H_{c2} are consistent with this predicted unusual dependence. Both the enhancement in H_{c2} and the critically pinned flux make such MgB_2 films more promising for applications, besides providing a cleaner and more intrinsic view of a superconductor's current-voltage response in the mixed state.

ACKNOWLEDGMENTS

---

*URL: http://www.physics.sc.edu/kunchur; Electronic address: kunchur@sc.edu

†Also at Instituto de Física, Universidad Autonoma de San Luis Potosí, S.L.P. 78000 Mexico.

[1] M.N. Kunchur, D.K. Christen, C.E. Klabunde, and J.M. Phillips, Phys. Rev. Lett. **72**, 752 (1994).

[2] M.N. Kunchur, Mod. Phys. Lett. B **9**, 399 (1995).

[3] A.V. Sologubenko *et al.*, Phys. Rev. B **65**, 180505(R) (2002); O.F. de Lima, R.A. Ribeiro, M.A. Avila, and A.A. Coelho, Phys. Rev. Lett. **86**, 5974 (2001).

[4] M.N. Kunchur, D.K. Christen, and J.M. Phillips, Phys. Rev. Lett. **70**, 998 (1993).

[5] W.N. Kang *et al.*, Science **292**, 1521 (2001).

[6] W.N. Kang *et al.*, Physica C **385**, 24 (2003).

[7] S.K. Gupta *et al.*, Physica C **206**, 335 (1993), and references therein; M. Nahum *et al.*, Appl. Phys. Lett. **59**, 2034 (1991), and references therein.

[8] M.N. Kunchur, Phys. Rev. Lett. **89**, 137005 (2002).

[9] M.N. Kunchur, B.I. Ivlev, D.K. Christen, and J.M. Phillips, Phys. Rev. Lett. **84**, 5204 (2000).

[10] O.M. Stoll, S. Kaiser, R.P. Huebener, and M. Naito, Phys. Rev. Lett. **81**, 2994 (2001).

[11] M.N. Kunchur, S.I. Lee, and W.N. Kang, Phys. Rev. B **68**, 064516 (2003).

[12] The value of the current density at which this jump occurs, $\sim 2 \times 10^7$ A/cm^2, is roughly comparable to the theoretical estimate of $j_d(0) = cH_c(0)/[3\sqrt{6}\pi\lambda(0)] \sim 6 \times 10^7$ A/cm^2.

[13] N.R. Werthamer, E. Helfand, and P.C. Hohenberg, Phys. Rev. **147**, 295 (1966).

[14] A. Gurevich, Phys. Rev. B **67**, 184515 (2003).

[15] Sometimes large departures can occur for exceptional situations such as superclean systems and narrow vortex cores where the internal energy-level spacing exceeds their widths.

[16] A.I. Larkin and Yu.N. Ovchinnikov, Zh. Éksp. Teor. Fiz. **68**, 1915 (1975) [Sov. Phys. JETP **41**, 960 (1976)].

[17] The slight shift in plateau resistance at the highest fields can be understood in terms of spreading of resistance outside the bridge area and into the current-lead areas as explained in the experimental section. Fields approaching H_{c2} start driving the whole film normal at relatively low currents so that the resistance of the wider current-lead areas is not frozen out. This causes the normal-state plateau to rise slightly at the highest fields.